Pyrolysis of Oil Shale: Experimental Study of Transport Effects

M. A. GALAN
and
J. M. SMITH
University of California
Davis, CA 95616

The thermal decomposition of kerogen in a Colorado shale was studied in a TGA-type apparatus in which the temperature was first increased at a constant rate and then held constant at a plateau value. Data were obtained at plateau temperatures from about 573 to 703 K and at 101.3 kPa.

The objective of the research was to determine the influence of transport effects on the observed rate of decomposition. The results show that, for the shale studied, transport of heat and mass influenced the rate, if the particle size was greater than about 0.4×10^{-3} m and if more than two to three layers of particles were placed in the weighing basket.

SCOPE

The production of oil from shale by thermal decomposition is a complex process, since the numerous chemical compounds in the kerogen and the sequence of pyrolysis reactions which they undergo are unknown. Hence, formulation of equations for the rate of decomposition is a difficult task. In addition to the problems associated with the intrinsic kinetics of the reactions, there is the possibility that finite transport rates for mass and energy may affect the observed or global rate.

Studies of kerogen decomposition have usually been carried out in thermal gravimetric type analyzers (TGA). The temperature is gradually increased or held constant, during which time weight is measured as the kerogen decomposes. The products leave the apparatus as vapors. In some cases these products flow through condensers so that the liquid oil production can be measured.

The objective of our work was to study experimentally (with an Anvil Points, Colorado shale) the effects of mass and heat transfer rates on the global rate of decomposition. A TGA-type apparatus was used to measure weight vs. time during, first, a linearly-increasing temperature period and then a subsequent constant-temperature period. Measurements were made for various particle sizes, nitrogen flow rates through the reactor holding the weighing basket containing the particles, and sample masses. No attempt was made to evaluate intrinsic rates. Our goal was to operate at conditions where the effects of transport effects could be observed without the intrusion of intrinsic kinetics.

CONCLUSIONS AND SIGNIFICANCE

It was found that three transport effects could affect the observed rate: 1) intraparticle, 2) particle-to-bulk fluid, and 3) interparticle. This conclusion was reached from the experiments with different particle sizes, nitrogen flow rates, and sample masses. The more fundamental factors studied by measuring sample mass is probably the number of layers of particles in the basket of fixed size. Mass and energy transport rates were not separated. However, for this one-reactant (kerogen) system (N_2 is an inert), it seems likely that heat transfer is more important than mass transfer. Quantitative investigation of the relation between heat and mass transfer by comparison of models with experimental results is planned for future studies.

For our shale at plateau temperatures from 573 to 703 K, the three transport processes did not affect the global rate when the particle size was about 0.4×10^{-3} m or less, the nitrogen flow rate was about 15×10^{-6} m^3/s or greater, and the number of layers of particles was no more than 2 to 3. The nitrogen flow corresponded to a superficial velocity in the reactor of about 2.1×10^{-2} m/s. This result is not of general significance since our apparatus (Figure 2) was designed to give a swirling motion to the entering nitrogen. This meant that a quantitative measure of turbulence in the gas around the particles was not possible. The experiments were carried out for the most part at a heating rate of 0.25 K/s. During the temperature-rise period, transport effects would be less important at lower heating rates. The heating rate should not change the conclusions based upon the constant-temperature period.

The significance of these results is that care must be taken with respect to particle size, gas flow rate, and sample size, in interpreting global rates of decomposition of kerogen in shale. Unless this is done, the observed rates will reflect transport effects, and rate equations based upon intrinsic kinetics controlling the pyrolysis process will be unrealistic.

THERMAL DECOMPOSITION OF OIL SHALE

Oil shale contains inorganic carbon (primarily as carbonates) and organic carbon in the form of compounds (called kerogen) containing carbon, hydrogen, nitrogen, oxygen and sulfur with small amounts of metals. Thermal decomposition occurs rapidly at temperatures above about 643 K to yield a relatively paraffinic oil as well as gases and char (carbon). The oil with suitable pretreatment, particularly for nitrogen removal, can be used as a refinery feed. At temperatures below 623 K pyrolysis is slow, as established in several prior investigations (Campbell et al., 1976a, 1976b; Shih and Sohn, 1980). At low temperatures there can be considerable desorption of water and gases.

Since the chemical structure of kerogen is complex and not well

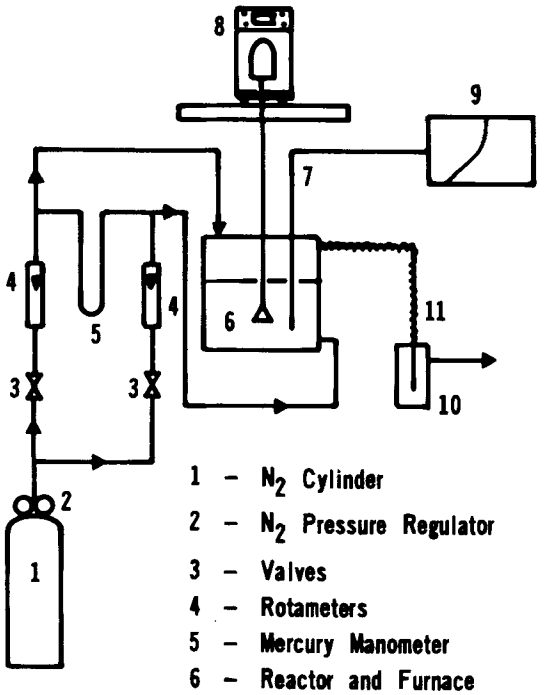

Figure 1. Pyrolysis apparatus.

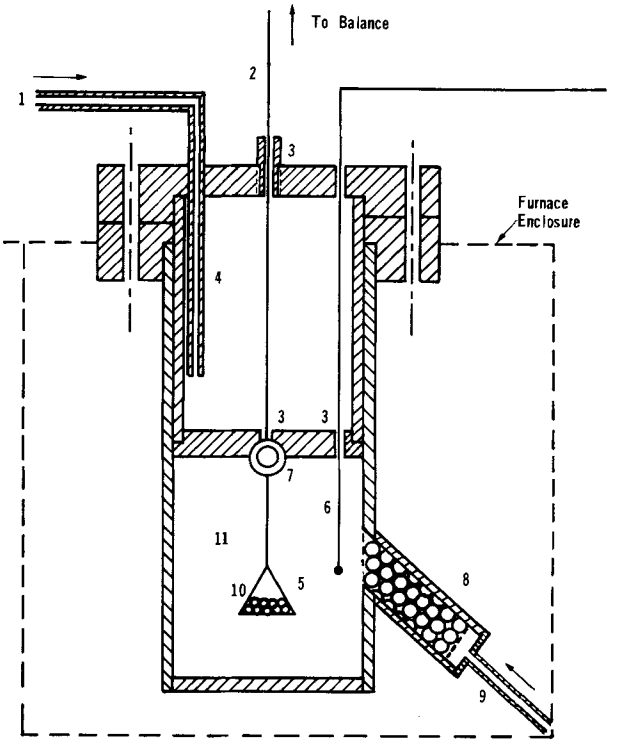

Figure 2. Reactor.

established, rates of thermal decomposition have been interpreted by simple overall reactions. One common view is that kerogen is a cross-linked, high molecular weight solid, and that during pyrolysis bonds are broken leading to bitumen. Hubbard and Robinson (1950) correlated their global rate data in terms of a two-step process, consisting of two first-order reactions:

$$\text{kerogen(s)} \rightarrow \text{bitumen} \quad (1)$$

$$\text{bitumen} \rightarrow \text{oil} + \text{gas} + \text{char} \quad (2)$$

where the bitumen product refers to lower molecular weight components which are vaporizable. Campbell and colleagues (1976a, 1976b, 1979) and Nuttall and coworkers (1977, 1979) have presented extensive kinetics data, and recognizing the complexity of the mechanism of decomposition, have analyzed the results with pseudofirst-order equations. Arnold (1975) and Shih and Sohn (1980) have also employed first-order expressions for the rate of oil generation. Braun and Rothman (1975) reanalyzed the Hubbard and Robinson data by introducing an induction period and reported rate constants and activation energies for each step in the two-step process. Johnson et al. (1975) introduced a more complex, ten-reaction mechanism for analysis of existing data and summarized activation energies reported by different investigators. The experimental data employed in these studies were obtained with different particle sizes and different gas flow rates around the particles. Both isothermal and nonisothermal operating conditions have been utilized, usually in Thermal Gravimetric Analyzers (TGA).

In these prior studies the observed global results were interpreted in terms of chemical kinetics, that is, by equations for the rates of chemical reactions occurring during decomposition. Our objective was to determine the extent to which transport processes affected global rates. Hence, rates were measured over a range of particle sizes (2.7×10^{-4} m to 4×10^{-3} m) and gas flow rates. A TGA apparatus was used and data obtained for different simple masses. This variable has been observed (Chihara et al., 1981) to affect TGA results, presumably due to the intrusion of interparticle transport effects (e.g., heat-transfer resistances). Most data were taken for the smaller particle sizes, larger gas flow rates, and smaller sample masses, to see for what conditions transport effects could be eliminated.

The sample weight was measured, both while the temperature was increased at a constant rate and afterwards when it was held constant at a chosen value. With this procedure and with a modest rate of temperature rise, the conditions where transport effects begin to influence the rate of kerogen decomposition could be established without the intrusion of intrinsic kinetics.

EXPERIMENTAL

Apparatus

The main items of the apparatus, as shown in Figure 1, are the furnace and reactor (6), and the analytical, weigh-through balance (8). Auxiliary items provided for a known flow of N_2 through the reactor containing the sample of shale particles and for temperature measurement.

The reactor system (Figure 2) is similar to that used for studying gas-solid, noncatalytic reactions as described by Costa and Smith (1971). The reactor chamber itself (11) consists of a 5×10^{-2} m tube approximately 7×10^{-2} m long. Nitrogen is fed at an angle through a packed-bed preheater (2×10^{-2} m ID, 5×10^{-2} m long) packed with 0.48×10^{-2} m stainless-steel balls). The inlet and exit are designed to provide extensive mixing around the screen basket holding the sample. The entire reactor system is of Monel 400. The basket and sample were weighed by a wire passing through pinholes (3) from the reactor chamber through a pressure chamber (4). A small flow of nitrogen passed continually through the pinholes into the reactor and out into the atmosphere. This nitrogen flow into the reactor chamber prevented pyrolysis products from passing through the lower pinhole. The pressure chamber prevented air from entering the reactor from the surroundings. The entire assembly was enclosed in a furnace up to the upper pinhole. The reactor temperature was measured with an iron-constantan

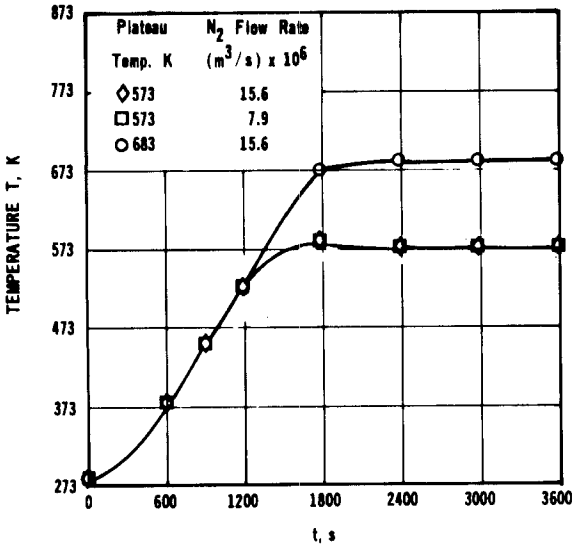

Figure 3. Thermal characteristics of furnace-reactor assembly.

thermocouple, controlled to ±2 K with a external Omega M-22 controller in the power line to the furnace, and recorded.

The basket holding the shale sample was formed from 316 stainless-steel screen with square openings of $0.41 \times 10^{-}$ m and wire diameter of 0.25×10^{-3} m (for the smallest particles a thin film of aluminum was placed inside the basket screen). The diameter of the basket itself was about 3×10^{-2} m. The weighing wire (diameter = 0.5×10^{-3} m), attached to the basket, was connected to the plate yoke underneath a Mettler H-6 digital readout balance (sensitivity of 10^{-6} kg).

The shale was from Anvil Points Mine, Colorado, with the following composition in wt. %: carbon 21.7, hydrogen 2.38, nitrogen 0.66, sulfur 0.66, moisture 0.50, and 23.3 wt. % inorganic carbonates. The density was 2.06×10^3 kg/m^3 at 298 K with a Fischer Assay of about 1.1×10^{-4} m^3/kg or 27 gal oil/(ton of shale). The granular particles as received (average size about 9×10^{-2} m) were crushed and sieved to provide granular samples. A diamond saw was used to cut the larger rectangular parallelepiped particles.

PRELIMINARY STUDIES—PROCEDURE AND REPRODUCIBILITY

Preliminary Experiments

To test reproducibility of the thermal characteristics of the furnace and reactor, preliminary runs were made without shale in the basket and for two different nitrogen flow rates and two plateau temperatures, T_f, of 573 and 683 K. As shown in Figure 3 reproducibility was good (to ±2 K) and a constant final temperature could be maintained. These runs were made at the approximately constant heating rate of 0.25 K/s.

Decomposition of inorganic carbonates was studied in additional preliminary runs by analyzing effluent gas samples in a chromatograph and by passing these gases through a barium hydroxide solution. These measurements indicated that carbon dioxide was produced beginning at a temperature of about 723 K, in agreement with the results of Campbell et al. (1976a, b) for the temperature at which the carbonates in western shale begin to decompose. Since kerogen pyrolysis was the subject of this study, TGA data was obtained up to a maximum of 703 K.

Procedure and Reproducibility

To start a run, shale particles were placed in the basket and nitrogen passed through the reactor for 900 s at room temperature (about 293 K) to remove weakly adsorbed gases and water). The temperature controller was set at the prescribed plateau temperature and the furnace and auxiliary apparatus turned on. Temperature and weight of shale sample (plus basket, holder and wire) were recorded during the temperature-rise period and for several thousand seconds after the constant temperature (574–703 K) was attained. This time was determined by the imposed requirement that the weight remain constant for 2,700 to 3,600 s. At the end of some of the runs the temperature was increased to 703 K to decompose completely the kerogen.

Three runs were made at the same conditions to check reproducibility. When the three sets of results did not agree, perhaps due to small differences in sample composition, a fourth run was made. The data at plateau temperatures less than about 623 K were influenced by the gases and water desorbed since the decomposition of shale is slow at these low temperatures.

As a test of overall weight changes, the shale sample was weighed before adding it to the basket, and after removing it from the basket when the run was over. The weight difference was within ±5% of the total weight change measured in the TGA-type apparatus.

TABLE 1. RANGE OF MEASUREMENTS

Particle Size	0.27×10^{-3} m (48 to 60 mesh) granular 0.42×10^{-3} m (32 to 42 mesh) granular 1.08×10^{-3} m (14 to 16 mesh) granular 2.25×10^{-3} m (7 to 12 mesh) granular 4×10^{-3} by 4×10^{-3} by 24×10^{-3} m parallelepiped (Kerogen layers perpendicular to the 24×10^{-3} m dimension)
Nitrogen Flow Rate (298 K, 101 kPa)	2.5×10^{-6} to 25×10^{-6} m^3/s
Sample Mass	0.25 to 1.36×10^{-3} kg
Heating Rate (for Ascending Temp. Data)	0.13 and 0.25 K/s
Plateau Temperature	573 to 703 K

RANGE OF MEASUREMENTS

Data were obtained for granular particles of four average sizes and for one parallelepiped as shown in Table 1. Nitrogen flow rate, mass of sample placed in the basket, and heating rate and temperature levels are also given.

RESULTS

Qualitative Weight vs. Time Curves

Before examining the experimental data it is instructive to consider the form of the weight vs. time curves. First, suppose that all transport effects are insignificant and that the decomposition reactions are zero order in kerogen. The constant-temperature data, for example in Figure 7, indicate that there is a fixed fraction of kerogen decomposed at each temperature. Hence, the weight of sample attains a constant value at long times. Under these restrictions the qualitative form of the curves are as shown in Figure 4. The weight w_1 corresponds to the constant weight associated with temperature T_1. The rate of decomposition is given by

$$\frac{dw}{dt} = -A \exp(-E/RT) \tag{1}$$

If the rate is low, the weight vs. time relation during the rising temperature period will be as shown by the solid curve (1) in Figure 4. During the constant-temperature period, the weight will fall linearly with time as shown by the dotted portion of curve (1). After w_1 is reached, the weight does not change further with time. At a higher rate the relation will be as shown by curve (2).

Suppose during the rising-temperature period that the rate of decomposition is extremely fast with respect to the rate of temperature rise. Then a specific fraction of kerogen would be decomposed at each temperature. If this relation is designated as $f(T)$, the weight vs. time curve would be

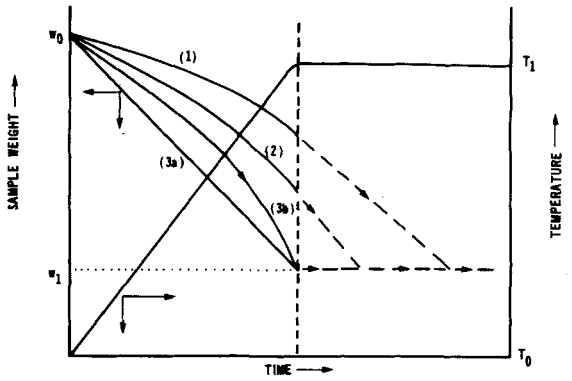

Figure 4. Qualitative weight and temperature vs. time curves for zero-order rate of decomposition and no transport effects [1-slow reaction rate; 2-faster reaction rate; 3a-instantaneous rate with $f(t) = aT$; 3b-instantaneous rate with $f(T) = -b_1 \exp(b_2 T)$].

$$w = w_o - w_o f(T) \tag{2}$$

and the rate is given by

$$\frac{dw}{dt} = -w_o \left[\frac{df(T)}{dT}\right] \frac{dT}{dt} \tag{3}$$

Since dT/dt is a constant, β, Equation 3 may be written

$$\frac{dw}{dt} = -w_o \beta \frac{df(T)}{dT} \tag{4}$$

Suppose there is a linear relation between $f(T)$ and T. Then $df(T)/dT$ is a constant, and the straight line shown in Figure 4, (3a), would result. At the constant temperature T_1 no further decomposition would occur so that the line in Figure 4 is horizontal after T_1 is reached. If the relation between $f(T)$ and T is exponential,

$$f(T) = b_1 \exp(b_2 T), \tag{5}$$

the rate equation during the rising-temperature period is given by

$$\frac{dw}{dt} = -w_o \beta b_1 b_2 \exp(b_2 t) \tag{6}$$

The weight vs. time relation for this case would be as shown by the (3b) curve in Figure 4.

For a first-order decomposition the weight vs. time curves would flatten out and reach w_1 asymptotically rather than sharply as shown in Figure 4. Equation 1 becomes

$$\frac{1}{w}\frac{dw}{dt} = \frac{d(\ln w)}{dt} = -A \exp[-(E/RT)] \tag{7}$$

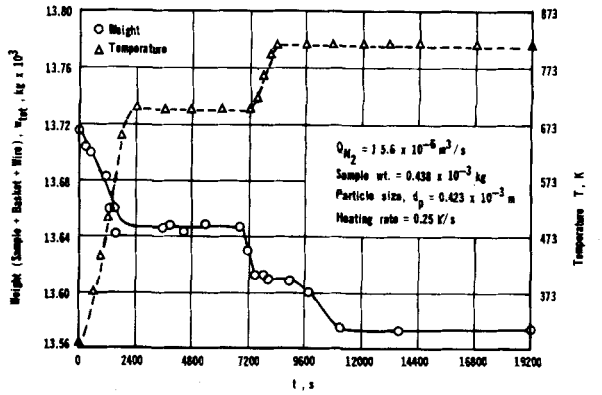

Figure 5. TGA data for small particles.

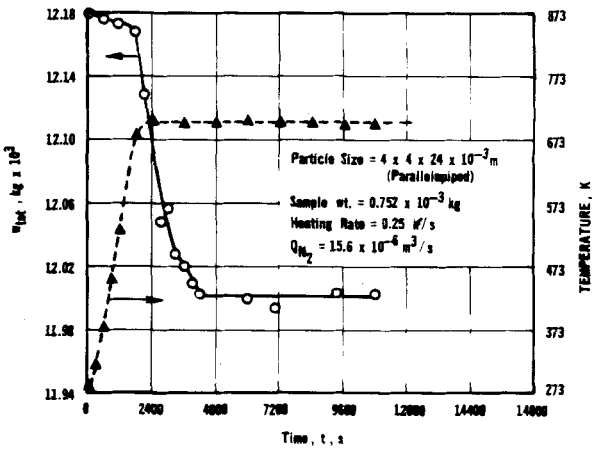

Figure 6. TGA data for large particles.

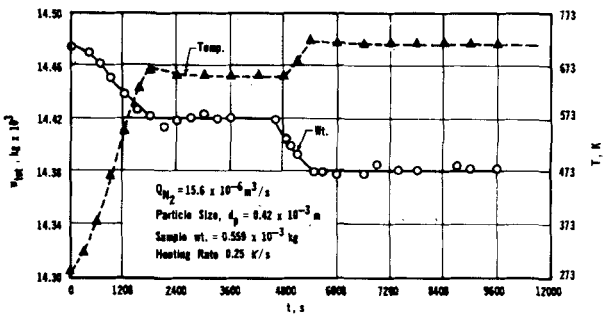

Figure 7. TGA data for two plateau temperatures.

Experimental Weight vs. Time Curves

Figure 5 shows experimental temperature and weight data for small particles, a high nitrogen flow rate, and a small sample mass (one to two layers of particles in the basket), and a plateau temperature of 698. As seen later, at these conditions there is no measurable retardation of the rate due to transport processes. The significant aspect of the weight curve is that the weight does not change after the temperature reaches 698 K. Such behavior corresponds to curves (3) in Figure 4 rather than (1) or (2). While more evidence is discussed later, this result suggests that, within the time scale of our experiments, the intrinsic rate of decomposition is too fast to measure. Hence, the goal has been achieved of operating at conditions where any deviation from constant weight is due to transport effects. Although no decomposition occurs at the constant temperature of 698 K, when the temperature is increased above 698 K decomposition proceeds (the weight decreases). This suggests that the maximum decomposition of kerogen at a given temperature is achieved within a few hundred seconds.

Figure 6 is for the same conditions as Figure 5 except a large particle ($4 \times 4 \times 24 \times 10^{-3}$ m parallelepiped) was placed in the basket. In this case the weight continues to decrease for several thousand seconds after the plateau temperature of 698 K is attained. This result shows that transport processes are reducing the rate, since changing particle size with other conditions constant could influence heat and mass transfer processes but not intrinsic kinetics of the decomposition reactions. The further decrease in weight, Figure 5, when the temperature is increased to the high value of 813 K is due in part to decomposition of carbonates.

Figure 7 presents data showing that the maximum decomposition depends upon the temperature. In this run the temperature controller was first set at 653 K, and after this temperature had been attained for several thousand seconds the controller was reset at the plateau of 713 K. Both of these temperatures are well below that at which carbonate decomposition occurs. The figure indicates that decomposition occurs during the temperature-rising periods, but not at either constant temperature level. The decrease in weight on heating from 653 to 713 K shows that all the kerogen was not

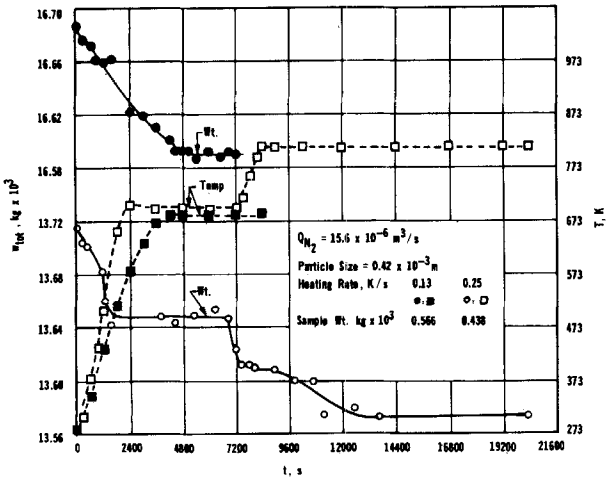

Figure 8. TGA data for two heating rates.

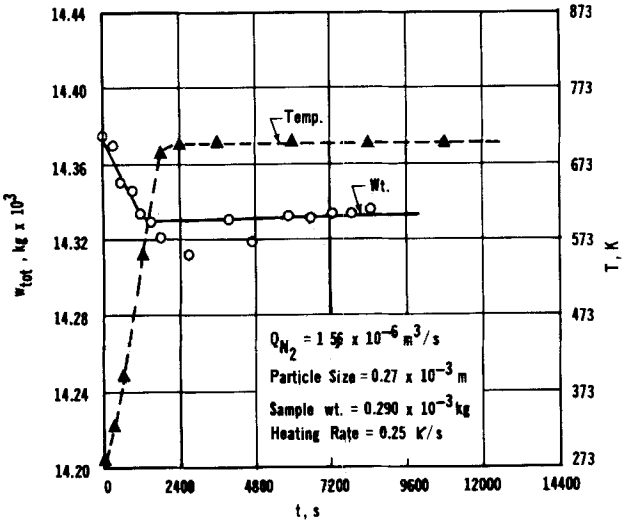

Figure 9. TGA data for smallest particles.

TABLE 2. FRACTION α OF KEROGEN DECOMPOSED AT DIFFERENT PLATEAU TEMPERATURES

Temperature K	Fraction Decomposed $\alpha = (w_o - w)/w_o$
573	0.07-0.09[a]
643	0.10
693	0.16
793	0.27[b]

[a] At temperatures of 573 K or lower, the fraction decomposed consisted partially of desorbed gases and water rather than pyrolysis products. Values of α showed deviations from run to run.
[b] Includes decomposition of some inorganic carbonates.

decomposed at 653 K, even after several thousand seconds at this temperature. Hence, complete decomposition can not explain the constant weight when the temperature was held at 653 K. The complex structure of kerogen and its numerous components, including strongly adsorbed gases and water, could provide an explanation. The decomposition reactions are probably irreversible, but the rates of decomposition and desorption for various components could be different. Hence, one type of component could be completely decomposed at a relatively low temperature, while the more refractory components have not reacted appreciably. In addition, some of the molecules may decompose in steps, with the first step producing some vaporized products at a low temperature and subsequent steps occurring only at higher temperatures.

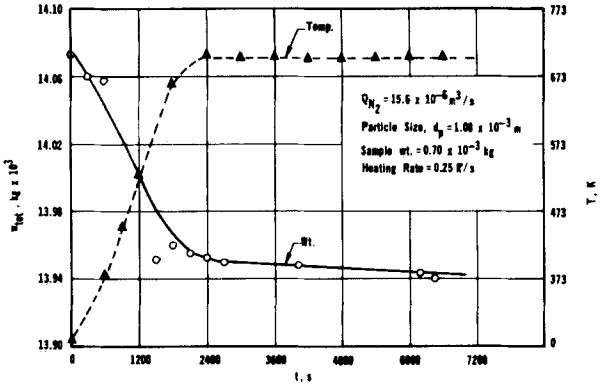

Figure 10. TGA data for 1.08 × 10^{-3} m particles.

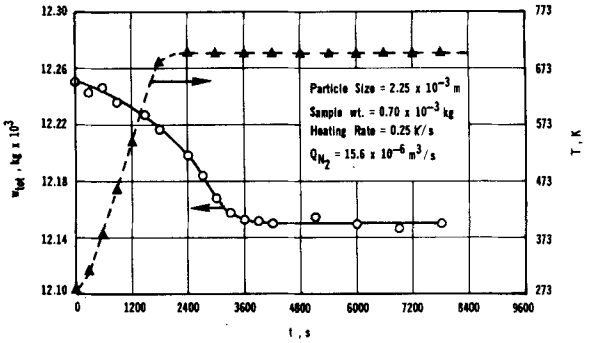

Figure 11. TGA data for 2.25 × 10^{-3} m particles.

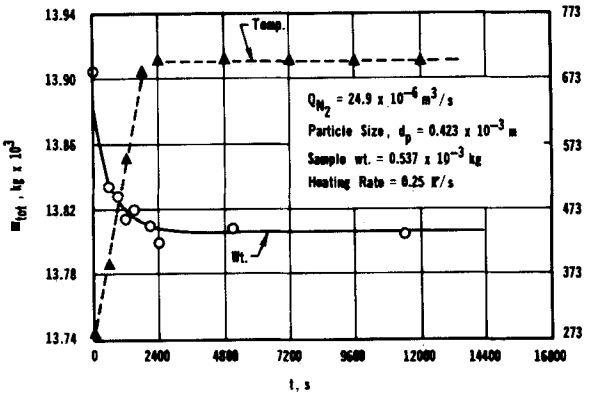

Figure 12. TGA data for highest nitrogen flow rate.

Similar results are observed when the heating rate is reduced. Figure 8 shows curves for 0.13 and 0.25 K/s with plateau temperatures 683 and 693 K, respectively. Higher heating rates were not desirable. Thus, at high rates the weight could continue to decrease after the plateau temperature is reached, due to the finite kinetics of the intrinsic reactions. Then it would not be possible to distinguish between transport effects and intrinsic kinetics.

Table 2 provides the relation $f(T)$ between the fraction (average for all runs) of kerogen decomposed and the temperature established by these data. The TGA measurements at plateau temperatures less than about 643 K showed considerable deviation from run to run. At these low temperatures the pyrolysis of shale proceeds very slowly and the weight change was due in part to desorption of gases and water. Hence, the effects of transport processes on the decomposition rate, Figures 9–14, are for plateau temperatures of 643 K or larger. The results in Table 2 should be specific for the shale used in our experiments but independent of transport effects and intrinsic kinetics. It is concluded from the data in Figures 5 and 7 that, when transport effects are not significant

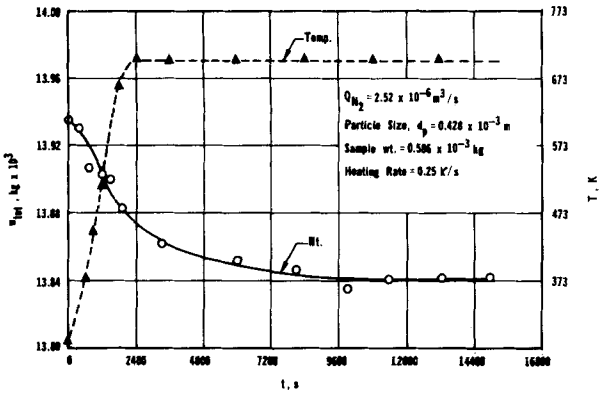

Figure 13. TGA data for lowest nitrogen flow rate.

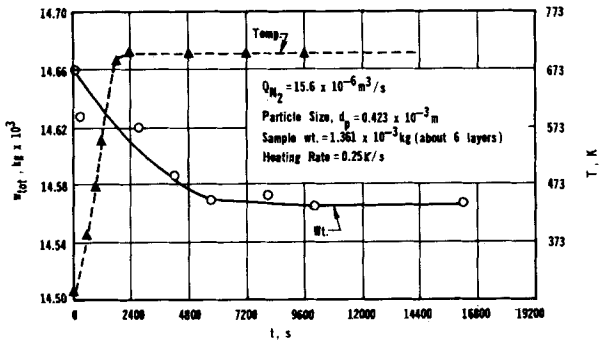

Figure 14. TGA for large sample weight.

and for a plateau temperature ≥643 K and heating rate ≤0.25 K/s, the intrinsic rate is too high to measure with our apparatus. The next step is to identify the conditions at which transport effects begin to be significant, that is, begin to reduce the global rate.

INTRUSION OF TRANSPORT EFFECTS

In our experiments there are three transport processes that may influence the global rate: 1) intraparticle transport which is affected by particle size; 2) particle-to-fluid transport which depends upon nitrogen flow rate and particle size; and 3) interparticle transport which depends upon the number of layers of particles in the sample basket. For a fixed particle size and for one basket, the third process can be studied by varying sample mass. Figures 9–14 show that transport effects do not influence the global rate of decomposition when the particle size is reduced to 0.42×10^{-3} m, when only two layers of particles are in the basket (corresponding to a mass of about 0.6×10^{-3} kg for 0.42×10^{-3} m particles), and when Q_{N_2} is 15.6×10^{-6} m^3/s or larger.

Heat transfer rather than mass transfer is regarded as most likely to be responsible when transport effects do reduce the global rate.

Particle Size

Figures 5 and 6 indicate that, for Q_{N_2} of 15×10^{-6} m^3/s and sample mass $\leq 0.7 \times 10^{-3}$ kg, transport processes retard the decomposition for the 4×10^{-3} m parallelepiped but that there are no transport resistances for 0.42×10^{-3} m particles. Figure 9 is for smaller particles (0.27×10^{-3} m) and, as expected, the weight does not change with time at constant temperature. The sample mass in this run was reduced to about one-half the value in Figure 5 in order that the basket contain no more than two layers of particles. With this small mass there was some oscillation in weight values.

Figure 10 is for larger particles (1.08×10^{-3} m) and here the sample weight continues to decrease (although only by a small amount) after the constant temperature of 693 K is attained. For larger particles (2.25×10^{-3} m), Figure 11 shows a larger weight decrease after the plateau temperature is reached.

From the data in Figures 5, 6, 9 and 10 it is concluded that in our apparatus intraparticle transport resistance begins to retard the global rate when the particle size reaches 1.0×10^{-3} m.

Nitrogen Flow Rate

Figures 12 and 13 display weight vs. time data for nitrogen flow rates larger and lower than the standard value of 15.6×10^{-6} m^3/s. The particle size (0.42×10^{-3} kg) and number of layers (about 2) are those which have been found to avoid transport affects. Figure 12 for a larger Q_{N_2} shows the same constancy of weight (after the plateau temperature is reached) that was found at $Q_{N_2} = 15.6 \times 10^{-6}$ m^3/s (Figure 5). However, when the flow rate is reduced to 2.52×10^{-6} m^3/s (Figure 13) the weight falls continuously after the plateau temperature is attained. We conclude that in our apparatus particle-to-fluid transport begins to retard the global rate when Q_{N_2} is between 15.6 and 2.52×10^{-6} m^3/s. These flow rates serve as critical values only for our reactor because the turbulence around the particles is complicated by the swirling nature of the flow due to the entrance arrangement (Figure 2).

It is believed that the predominant transport limitation is due to heat transfer. Estimates of heat and mass transfer coefficients, along with the experimental rates (dw/dt values), estimated heat of decomposition and physical properties, gave negligible concentration differences between bulk nitrogen and particle surface while corresponding temperature differences were 1 to 10 K, depending on gas flow rate and particle size. To substantiate this conclusion, particle surface and particle center temperatures were measured (with thermocouples) as well as gas temperatures in a run with 4×10^{-3} m particles at a nitrogen flow rate of 2.5×10^{-6} m^3/s. The gas-to-particle temperature difference was 6 K while the intraparticle ΔT was 1 K.

Sample Mass (Number of Layers)

Figure 14 shows data for the small particles and high Q_{N_2} which have been found to avoid transport effects, but for a larger sample mass (six to seven layers of particles in the basket). The intrusion of transport resistance is evident by the decrease in weight after the temperature has reached the plateau value. Similar results were observed whenever the number of layers in the basket exceeded two or three. We believe this retardation of the rate is due to temperature gradients within the sample; that is, the temperature in the center of the sample experiences a delay in reaching the temperature at the outer edge of the sample.

Summary of Transport Effects

The effects of transport processes are summarized in Figure 15. This figure shows the fractional loss in weight of sample, α vs. time for a plateau temperature of 693 K. The upper curve corresponds to the conditions where no transport resistances have been observed; that is, conditions closely corresponding to those for Figure 5. The lower three curves show, separately, the effects of decreasing the nitrogen flow rate, increasing the particle size, and increasing the sample mass, w_o. At very long times all four curves would converge at the same α.

It is concluded that in TGA experiments care must be taken to exclude transport effects if intrinsic kinetics of shale decomposition are to be studied. The effects of particle size and gas flow rate are easily acceptable. The severe retardation due to number of layers of particles is less obvious. This effect is likely to be observed in thermobalance experiments where the sample mass is very small since the basket or pan in these devices is also very small. The most significant parameter is probably the number of layers of particles in the pan. In some of the reported TGA data, transport effects, particularly those due to sample mass and particle size, may have been important. When such data are analyzed in terms of kinetic

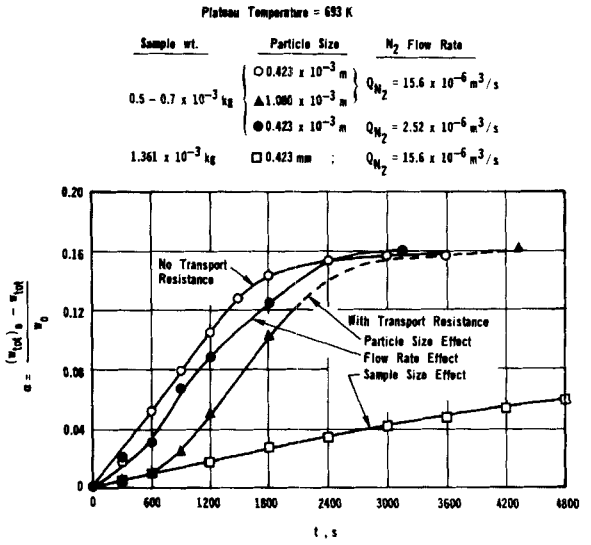

Figure 15. Effect of transport processes on fractional weight change, α.

equations (for example first-order rate expressions) it is important to note that the rate constants are not real kinetic constants but pseudo values.

ACKNOWLEDGMENT

The Fellowship provided by the Fulbright Commission and the financial assistance of National Science Foundation Grant CPE-8026101 are gratefully acknowledged. The Occidental Research Corp. kindly provided the shale and its elemental analysis.

NOTATION

A = preexponential factor, Eq. 1, kg/s
b_1, b_2 = constants in Eq. 5
E = average activation energy for an overall intrinsic rate equation for kerogen decomposition, J/kmol
d_p = diameter (ave.) of granular shale particles, m
$f(T)$ = fraction of kerogen decomposed at temperature T
R = gas constant, J/(kmol)(K)
T = temperature, K; T_f = plateau temperature
t = time, s
w = weight of shale sample, kg; w_o is the initial weight
w_{tot} = weight of sample + basket + wire, kg
Q_{N_2} = nitrogen flow rate, m^3/s
β = constant rate of temperature rise, K/s

LITERATURE CITED

Arnold, C. H., "Effect of Heating Rate on the Pyrolysis of Oil Shale," Paper #28, Symposium in Industrial and Laboratory Pyrolyses, Div. of Petroleum Chemistry, 169th ACS Mtg., Philadelphia (April 7–8, 1975).

Braun, R. L., and A. J. Rothman, "Oil Shale Pyrolysis: Kinetics and Mechanism of Oil Production," *Fuel*, **54**, p. 129 (1975).

Campbell, J. H., G. Koskinas, and N. Stout, "The Kinetics of Decomposition of Colorado Oil Shale: I. Oil Generation," Lawrence Livermore Laboratory, UCRL-52089 (1976a).

Campbell, J. H., "The Kinetics of Decomposition of Colorado Oil Shale: II Carbonate Mineral," Lawrence Livermore Laboratory, UCRL-52089, Part 2 (1976b).

Campbell, J. H., and A. K. Burnham, "Reaction Kinetics for Modeling Oil Shale Retorting," Lawrence Livermore Laboratory, UCRL-81622 (1979).

Chen, W. J., and H. E. Nuttal, "TGA Study of Colorado Shale and New Model for Pyrolysis," 86th AIChE National Meeting, Houston (1979).

Chihara, K., J. M. Smith, and M. Suzuki, "Regeneration of Powdered Activated Carbon. Part I. Thermal Decomposition Kinetics," *AIChE J.*, **27**, p. 214 (1981).

Costa, E. C., and J. M. Smith, "Kinetics of Non-catalytic, Non-isothermal Gas-solid Reactions: Hydrofluorination of Uranium Dioxide," *AIChE J.*, **17**, p. 947 (1971).

Granoff, B., and H. E. Nuttall, "Pyrolysis Kinetics for Oil Shale Particles," Fuel, **56**, p. 234 (1977).

Hubbard, A. B., and W. E. Robinson, "A Thermal Decomposition Study of Colorado Oil Shale," U.S. Bureau of Mines, Report of Investigation, #4744 (1950).

Johnson, W. F., D. K. Walton, H. H. Keller, and E. J. Couch, "*In Situ* Retorting of Oil Shale Rubble: A Model of Heat Transfer and Product Formation in Oil Shale Particle," Quarterly of Colorado School of Mines, **70**(3), p. 237 (1975).

Shih, S. M., and H. Y. Sohn, "Non-Isothermal Determination of the Intrinsic Kinetics of Oil Generation from Oil-Shale," *I & E.C. Process Des. Dev.*, **19**, p. 420 (1980).

Manuscript received March 11, 1982; revision received August 2, and accepted August 30, 1982.